SLAC-PUB-1729
March 1976

INELASTIC ELECTRON-NUCLEON SCATTERING EXPERIMENTS*

R. E. Taylor

Stanford Linear Accelerator Center
Stanford University, Stanford, California 94305

I. INTRODUCTION

The major topics in this report are based on new results from single arm inelastic electron scattering experiments by the MIT-SLAC (SFG) group[1] and by SLAC (Group A)[2]. Both of these analyses include hitherto unpublished data and give new information about the scaling of the nucleon structure functions. It is interesting to compare the present data on the reaction

$$e + p \rightarrow e' + \text{Anything}$$

with the predictions made almost a decade ago by Bjorken[3]. He conjectured that

$$\lim_{Q^2 \rightarrow \infty} \nu W_2(Q^2, \nu) = F_2(x) \tag{1a}$$

and

$$\lim_{Q^2 \rightarrow \infty} 2MW_1(Q^2, \nu) = F_1(x) \tag{1b}$$

where

$$x = \frac{1}{\omega} = \frac{Q^2}{2M\nu} \tag{2}$$

These relations will not hold in the resonance region where there are enhancements at particular values of W, nor for small Q^2, since $\nu W_2(0,W) = 0$. In the earliest inelastic electron experiments performed at SLAC the data obeyed relation (1a) to about 10% for $Q^2 > 1$ GeV^2, $W^2 > 4$ GeV^2.

Since that time a large amount of data has accumulated, and Fig. 1a shows values of νW_2 measured at SLAC over the past six years, taking $\epsilon > 1/2$, assuming $R = 0$, and with cuts of $Q^2 > 1$ GeV^2, $W^2 > 4$ GeV^2. Each value of νW_2 is plotted as a bar with vertical height corresponding to the assigned errors. [The large bars below $x = 0.3$ are data from a muon scattering experiment,[4] and the spread shown is due to a combination of Q^2 variation (non-scaling) and error bars on several overlapping data points at each value of x.] For the electron data the Q^2 range of the data plotted varies somewhat for different regions of x:

$x = 0.7$	$7 < Q^2 < 14$
0.5	$4 < Q^2 < 10$
0.35	$2 < Q^2 < 8$
0.2	$1 < Q^2 < 5$

*Work supported by the U. S. Energy Research and Development Administration.
(Invited paper presented at the International Symposium on Lepton and Photon Interactions, Stanford University, Stanford, California, August 21-27, 1975.)

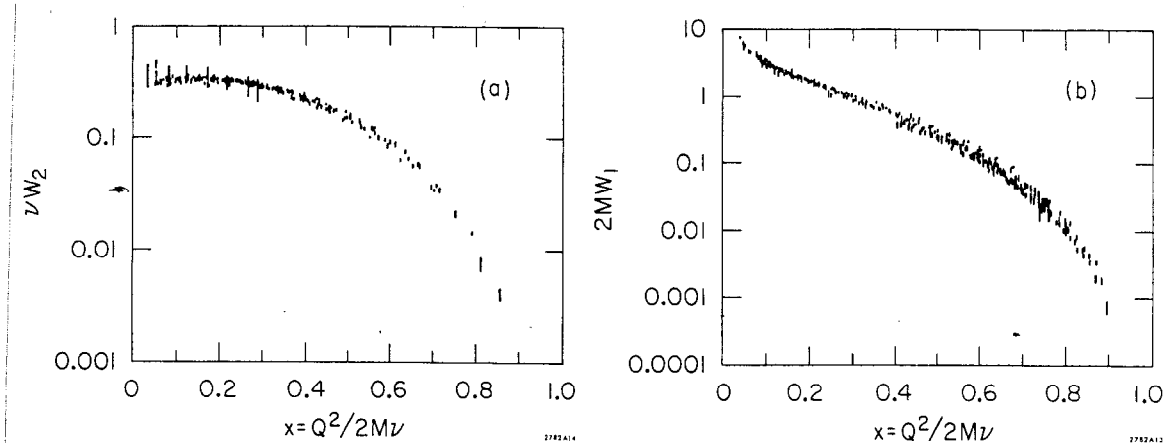

Fig. 1--Values of νW_2 and $2MW_1$ for the proton with $Q^2 > 1$ GeV^2 and $W^2 > 4$ GeV^2. $R = \sigma_L/\sigma_T$ is assumed to be zero, and values of νW_2 are extracted from cross section measurements with $\varepsilon \geq 1/2$, while values of $2MW_1$ are extracted for $\varepsilon \leq 1/2$. The large vertical bars below $x = 0.3$ in the graph of νW_2 are obtained from muon data taken at Fermilab.

A similar plot for $2MW_1$ is shown in Fig. 1b, where points with $\epsilon \leq 1/2$ are plotted. Here the Q^2 range is somewhat greater in most regions of x, and there is some obvious spread in the points. Nevertheless, the scaling relations still retain considerable predictive power since the maximum spread in the data is around 30% while Q^2 and ν each vary by well over an order of magnitude.

The study of the deviations from scaling is the main subject of each of the new analyses. There are several possible reasons why observations of the structure functions measured at finite values of Q^2 could show deviations from scaling and for which relations (1a) and (1b) would still hold in the limit of infinite Q^2. Examples are resonance contributions to the inelastic cross sections; additional terms in $F(x)$ which vary as $1/Q^2$ (one way to include such terms is by including terms of order $1/Q^2$ in the variable itself); and confusion in the analysis through ignoring the exchange of more than one photon in the interaction. In addition, there have been many theoretical suggestions which would modify Bjorken's conjectures and lead to limiting behavior quite different from that suggested in the relations (1a) and (1b). These suggestions include theories with anomalous dimensions, theories which are asymptotically free, the excitation of new degrees of freedom like charm or color, the possible existence of form factors for constituents in the parton model, and so on.

About five years ago, deviations from scaling were observed experimentally[5] for values of W^2 between 4 and 6 GeV^2, and scaling was repaired by a change in the scaling variable to $x' = 1/\omega'$ where

$$\omega' = \omega + M^2/Q^2 = W^2/Q^2 + 1 \qquad (3)$$

Since W and ν are both plausible invariants to use in constructing a scaling variable, and since ω' approaches ω in the limit as $Q^2 \to \infty$, there is little theoretical justification for preferring one variable over the other.

Simple models of scaling in the deep inelastic appeared to require that the ratio

$$R_A = \frac{e^+e^- \to \text{hadrons}}{e^+e^- \to \mu^+\mu^-}$$

in annihilation experiments should be constant with varying center-of-mass energy. The early results from CEA and then from SPEAR showing R_A rising with increasing center-of-mass energy focussed attention on possible scale breaking in the scattering experiments. At about the same time indications of scale breaking with $x < .03$ were reported[6] in the muon scattering experiments at Fermilab. At such low values of x the difference between x and x' is small, so that the muon data indicated scale breaking in $x'(\omega')$ for the first time. The evidence for breaking in the muon experiment is now somewhat stronger, as reported in the last talk.[7] This year the conflict between the behavior of R_A and theoretical predictions based on the scattering experiments has been attenuated by the discovery of the new particles, which may provide a rationale for the increase in R_A encountered around center-of-mass energies of 4 GeV.[8] The lepton-nucleon scattering should show the effects of any new thresholds as well, but there are no clear predictions of the magnitude and kinematic location of such effects.

II. STATUS OF ELECTRON SCATTERING RESULTS

The reaction

$$e + p(d) \to e' + X$$

in which only the recoiling electron is detected is still being intensively studied at SLAC, and analyses have been made on two separate data sets.[1,2] The MIT-SLAC(SFG) analysis is a comprehensive look at data for both large and small angle scattering including some hitherto unreported results. The SLAC (Group A) analysis is based on data from large angles only, since our new data for small angles are not yet available. Table I gives some of the details of the data sets used.

TABLE I

Data Set	SLAC Experiment Number	Scattering Angle θ (deg)	Spectrometers Used	Target	Incident Energy Range E_0 (GeV)	Polarization Parameter Range ε	Extracted Quantities
MIT-SLAC (SFG)	E49a E49b E87	6, 10 18, 26, 34 15, 19, 26, 34	20-GeV 8-GeV	H_2, D_2	4.5-19.5	0.24-0.98	R, νW_2, W_1
SLAC (Group A)	E89	50, 60	1.6-GeV	H_2, D_2	6.5-19.5	0.08-0.25	W_1

2782A35

A. MIT-SLAC(SFG) ANALYSIS

From the experimental yields at different values of E, E', θ this group obtains values of cross sections. After radiative corrections these cross sections are used to obtain values of a combination of the absorption cross sections for virtual photons:

$$\sigma_T(Q^2,W^2) + \epsilon\sigma_L(Q^2,W^2) = \frac{1}{\Gamma}\frac{d\sigma}{d\Omega\, dE'} \qquad (4)$$

where Γ is the flux of virtual photons. By interpolation the quantity on the left-hand side of Eq. (4) is obtained for given values of (Q^2,W^2,θ). From the variation of this quantity with

$$\epsilon = \{1 + 2(1 + \nu^2/q^2)\tan^2\theta/2\}^{-1}$$

one obtains values of

$$\sigma_L(Q^2,W^2) \quad \text{and} \quad \sigma_T(Q^2,W^2) \quad \text{and thus} \quad R(Q^2,W^2) = \sigma_L/\sigma_T$$

The cross sections have errors, and, in particular, there are systematic errors which must be carefully controlled in order to extract reliable results. The details of the analysis can be found in Ref. 1. Here I will only list typical errors on the cross sections:

$\sim \pm 2\%$	based on statistical counting errors
$\sim \pm 1\%$	systematic errors which are thought to vary in a more or less random fashion from data point to data point.
$\sim \pm 1-2\%$	systematic errors which may affect whole regions of the data, e.g., normalization between different experiments, various calibrations and efficiencies, radiative corrections, etc.
$\pm 4\%$	overall normalization which affects the structure functions but not the ratio R nor the ratio of deuterium and hydrogen cross sections.

The experimenters have chosen 75 points in the (Q^2,W^2) plane, and at each point they make a careful error analysis and separate the structure functions. The points themselves must be selected with care to equalize the contribution of the various cross section measurements and minimize correlated errors between neighboring separation points. The data cover a large range in x $(0.1 < x < 0.8)$ for values of Q^2 and W^2 as indicated in Fig. 2.

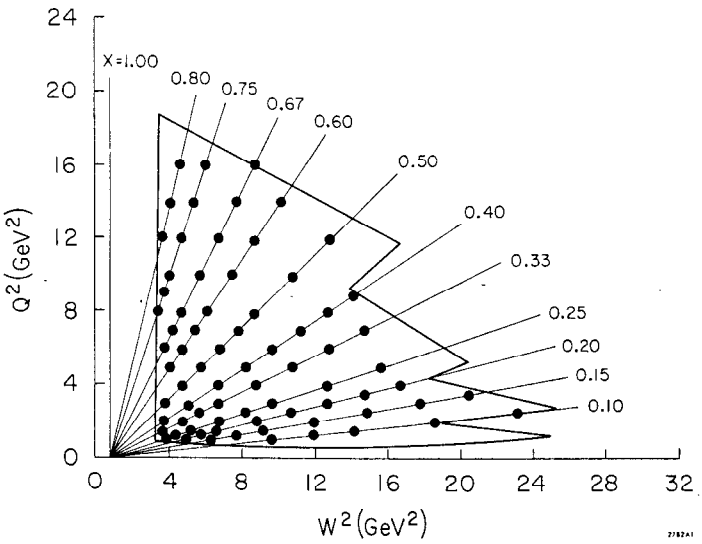

Fig. 2--Kinematic points chosen for structure function separation in Ref. 1. By choosing several points with the same value of the scaling variable x, the scaling of R_p and the structure functions can be tested in this variable.

ANALYSIS OF R_p

From data obtained using the hydrogen target, seventy-five measurements of R_p are obtained in this way. For simple models with spin 1/2 constituents, R_p should vanish as $1/Q^2$ (or $1/\log Q^2$ for asymptotically free theories). The results of this analysis are consistent with either limiting behavior, and are even consistent with R_p = constant. The value of the constant is given as 0.14 with a statistical error of $\pm$ 0.011 and a possible systematic error of $\pm$ 0.056. Figure 3 shows the values of R_p obtained for the different values of x shown in Fig. 2, together with fits of various functional forms. A full discussion of the possible x dependence of R_p is given in Ref. 1. The simplest fit, R = const. for each bin, would show R decreasing from ~ 0.3 for x = 0.1 to ~ 0.1 for x = 0.8, but the significance of this effect is not yet established, due to the presence of systematic errors and the possibility that R is not in the asymptotic region at the lower values of Q^2.

STRUCTURE FUNCTIONS FOR THE PROTON

The MIT-SLAC(SFG) analysis also gives 75 pairs of values for σ_T and σ_L or equivalently W_1^p and W_2^p. Figure 4 shows νW_2^p and $2MW_1^p$ for selected values of x. It is obvious that rather large violations of scaling are taking place in the variable x.

At this point I want to establish a simple scheme which will facilitate the discussion of scaling violations in different variables. It will turn out that there is no evidence that the observed violations in the electron data exhibit any x dependence. (This is not the case for the muon data.[4]) The electron data can be described quite well under the following assumptions:

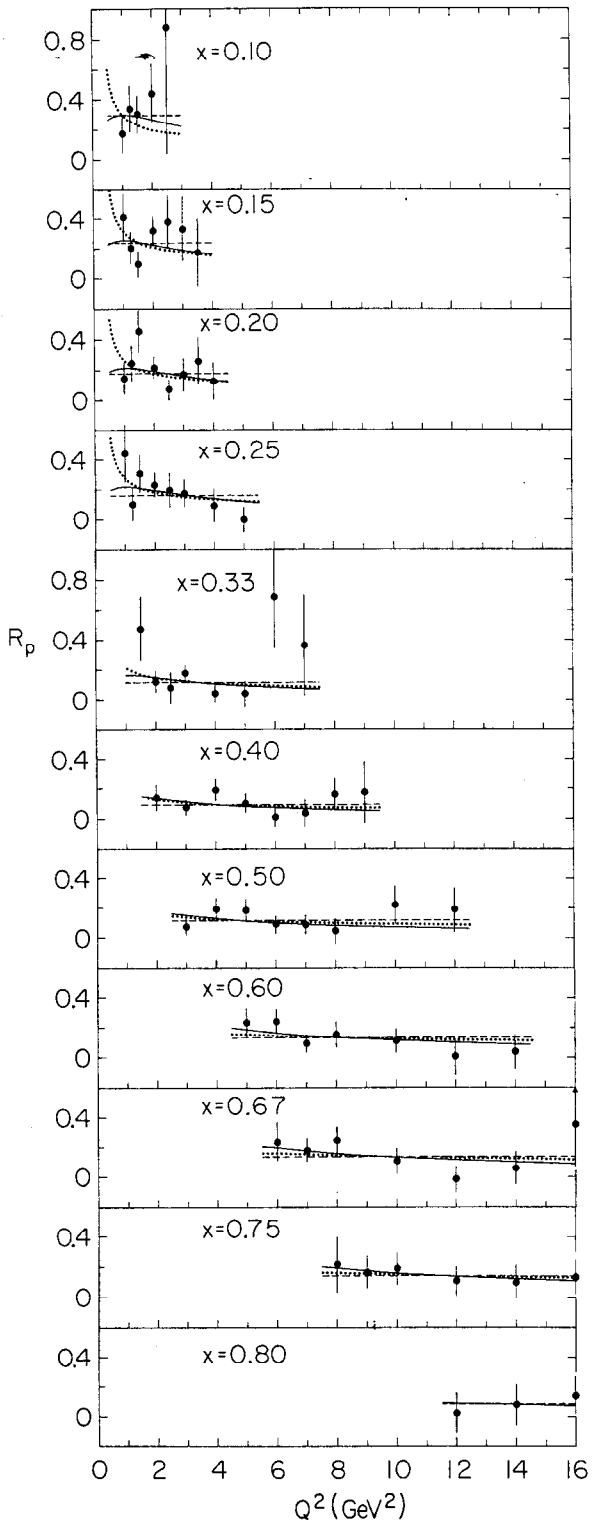

Fig. 3--Values of R_p for the points in Fig. 2. The dashed lines in the figure represent the best fit of the form R_p = constant to the data at a given value of x. The solid and dotted lines represent fits of the form

$$R = C(x) \frac{Q^2}{(Q^2 + d^2)^2} \quad \text{and}$$

$$R = \frac{\alpha^2(x)}{\ln(Q^2/\beta^2)}$$

respectively. There are some systematic sources of error in addition to the errors shown in the figure.

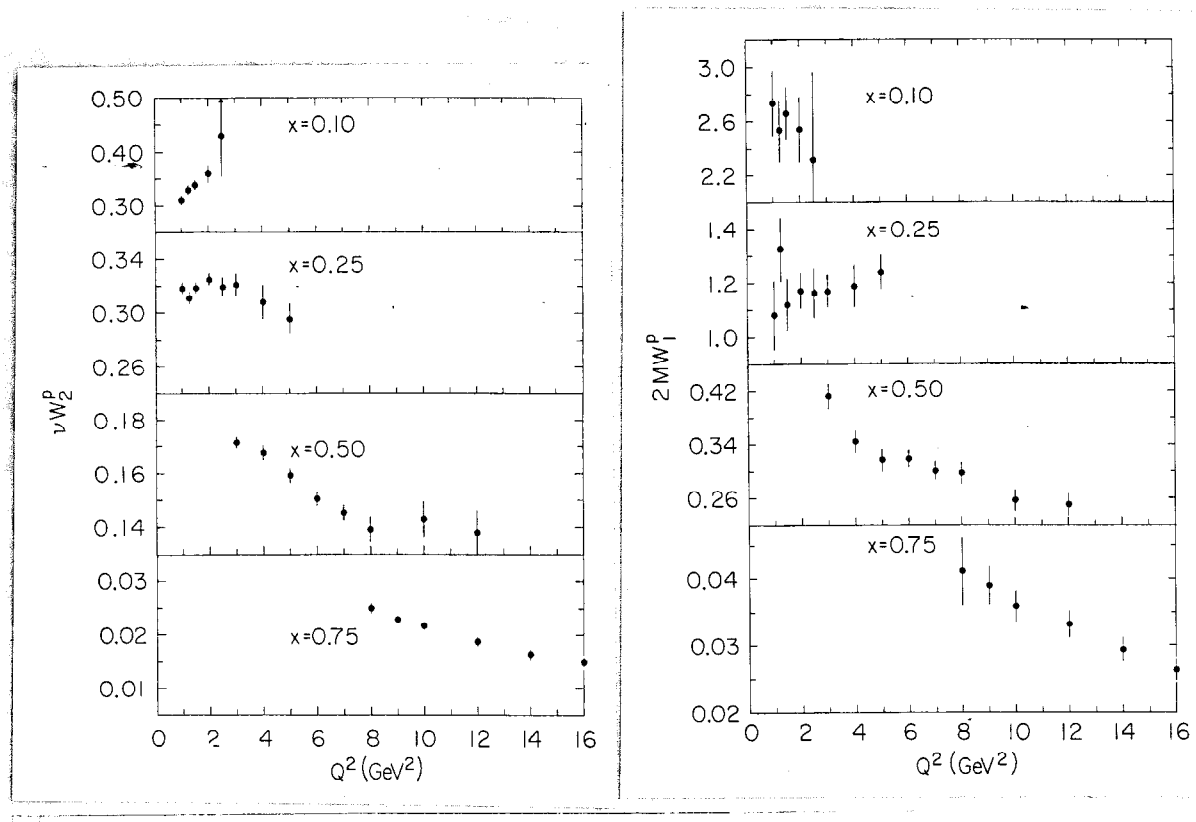

Fig. 4--νW_2^p and $2MW_1^p$ structure functions. Separated proton structure functions are illustrated for selected values of x. It is clear that neither structure function is scaling in x, i.e., that there is Q^2 dependence of the structure function at constant x.

(1) Assume scaling variables, x_a, of the form $1/x_a = \omega_a = \omega + a/Q^2$, where $\omega = 2M\nu/Q^2 = 1/x$ and a is a parameter $(x_0 = x,\ x_{M_p^2} = x',$ etc.).

(2) We allow scale breaking through a term which is linear in Q^2, say $(1 + bQ^2)$.

Then, we can write

$$\nu W_2(Q^2, W^2) = F_2(\omega_a)(1 + bQ^2) \tag{5}$$

F_2 is expressed as a power series in $(1 - x_a)$, e.g.,

$$F_2(\omega_a) = \sum_{i=3}^{i=7} \alpha_i (1 - x_a)^i \tag{6}$$

More complicated forms could be used for the variable, the breaking, or the functional form of F_2, but the present electron data do not really justify the use of more than a couple of parameters (a and b) to describe the breaking.

With this scheme, one can investigate the goodness of fit for various cases:

(a) Bjorken scaling: $a = b = 0$. It is obvious from Fig. 4 that this case will give a very poor fit to the data.

(b) Bjorken variable, $Q^2/2M\nu$, $a = 0$, b arbitrary. For νW_2: $b_2 = -0.028 \pm .001$ $(\mathrm{GeV})^{-2}$. A similar analysis applied to W_1 data gives $b_1 = -0.029 \pm 0.002$ $(\mathrm{GeV})^{-2}$. But χ^2 values for these "solutions" are still quite poor.

(c) Modified scaling variable, x'; $a = M_p^2$, $b = 0$: This choice of parameters gives a poor fit for νW_2 and a barely acceptable fit for W_1. This observation of non-scaling in x' is new and depends on the new data taken at 15°, 19°, 26° and 34°.

(d) For the variable x', $a = M_p^2$, b arbitrary: For νW_2: $b_2 = -0.011 \pm .001$. For W_1: $b_1 = -.009 \pm .004$.

The change in b from $3\%/(\mathrm{GeV})^2$ for the variable, x, to $1\%/(\mathrm{GeV})^2$ in x' illustrates the tradeoff between the scaling variable and breaking (i.e., between the parameters a and b).

In Fig. 4, the νW_2 data in the bin at $x = 0.1$ show a rise with increasing Q^2. Data at low x correspond to low values of Q^2. The MIT-SLAC (SFG) group points out that at $x = 0.1$ the νW_2 data are still in the "turn on" region, where Q^2 is less than $2\ (\mathrm{GeV})^2$. From previous experiments[9] it appears that νW_2 might decrease by as much as 8% between $Q^2 = 2(\mathrm{GeV})^2$ and $Q^2 = 1(\mathrm{GeV})^2$. The MIT-SLAC(SFG) group suggest that fits should include only data with $Q^2 > 2\ (\mathrm{GeV})^2$ in order to avoid such problems. In the past most fits have been made to data for $Q^2 > 1(\mathrm{GeV})^2$ and such fits should be corrected for the turn on effect.

B. W_1 FROM SLAC (GROUP A) EXPERIMENT

We have analyzed recent measurements[2] taken at 50° and 60° using the 1.6-Gev spectrometer. The kinematic region covered by these measurements is shown in Fig. 5, along with the parameters ω' and ϵ. It is the polarization parameter, ϵ, which, in combination with R, determines the relative contribution of σ_L and σ_T to the cross section (see Eq. 4). Small values of ϵ imply a small contribution from σ_L, and if in addition $R = \sigma_L/\sigma_T$ is small, the cross section depends mostly on σ_T (or W_1). Without approximation we can write

$$W_1 = \frac{d\sigma/d\Omega dE'}{\sigma_{\mathrm{Mott}}} \frac{1}{2\tan^2\theta/2} \frac{1-\epsilon}{1+\epsilon R} \tag{7}$$

In the region where the new data overlap the separation region of the MIT-SLAC (SFG) experiment (Fig. 5) we depend on their measurements of R. Outside this region, the small values of ϵ make the determination of W_1 insensitive to the details of extrapolation in R. We have assumed $R = 0.18$ everywhere.

W_1 and x

The results for W_1 are shown in Fig. 6. The scatter of the points suggests that the data may not scale in x. Figure 7 shows data with $0.5 < x < 0.7$ as a function of Q^2. Fits of the form

$$W_1(Q^2,W^2) = F_1(\omega_a)(1 + bQ^2) \tag{8}$$

where

$$F_1(\omega_a) = \sum_{i=3}^{i=7} \beta_i (1 - x_a)^i \tag{9}$$

(corresponding to Eqs. 5 and 6 for W_2) have been made. For the x variable ($a = 0$), the fits give large values of χ^2 per degree of freedom. It is clear from Fig. 7 that this will be the case, as the points don't lie on a straight line. To achieve a good fit in x we would require a more complicated scale-breaking function in Eq. 8.

W_1 and x'

In x', ($a = M_p^2$), the data are a poor fit to Eq. (8) with $b = 0$. If we fit for the best value of b with x' as a variable, we find

$$b_1 = -0.011 \pm 0.001 (\mathrm{GeV})^{-2}$$

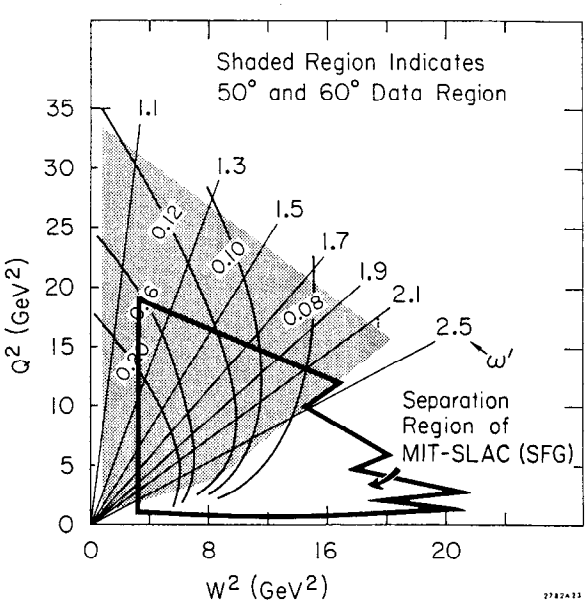

Fig. 5--Kinematic regions for 50° and 60° experiments. Data were obtained in the shaded region. Lines of constant ω' are shown along with lines of constant $\epsilon = \{1+2(1+\nu^2/Q^2)\tan^2\theta/2\}^{-1}$ for $\theta = 60°$. Values of $R = \sigma_L/\sigma_S$ have been obtained in the MIT-SLAC (SFG) analysis for the indicated regions.

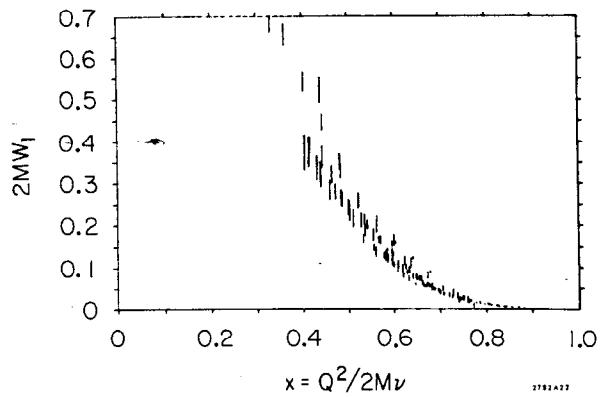

Fig. 6--Measurements of W_1 for the proton. Data from both 50° and 60° experiments and MIT-SLAC (SFG) analysis are shown for $\varepsilon \leq 1/2$. 50° and 60° data all have $x > 0.4$. Cuts are $Q^2 > 1$ GeV^2 and $W^2 > 4$ GeV^2.

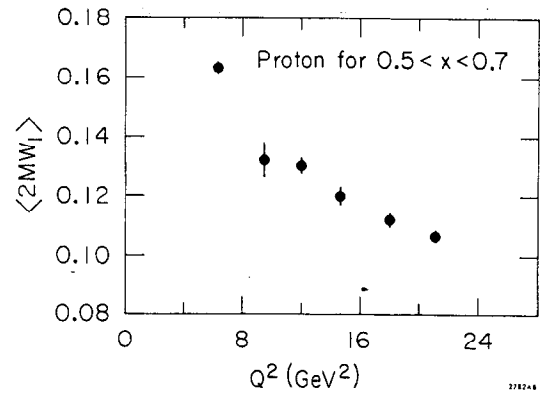

Fig. 7--Q^2 dependence of $2MW_1$ for the proton. Data from 50° and 60° in the range $0.5 < x < 0.7$ are used to obtain values of $2MW_1$ for six Q^2 bins between 7 and 20 GeV^2.

This is in agreement with the value of b_1 found by MIT-SLAC(SFG)[10]

$$b_1 = -0.009 \pm 0.004(\text{GeV})^{-2}$$

Perhaps more interesting is the close correspondence with the more accurate MIT-SLAC(SFG) measurement of the scale breaking of νW_2 in x'

$$b_2 = -0.011 \pm .001(\text{GeV})^{-2}$$

W_1 and x_s

In his thesis,[2] Atwood shows that a good fit to the W_1 data can be obtained with $b = 0$ and a arbitrary. He calls the resulting variable x_s:

$$1/x_s = \omega_s = \omega + 1.5 \text{ GeV}^2/Q^2$$

The actual fitted parameters for the 50° and 60° data are

$$a = 1.48 \pm 0.05(\text{GeV})^2$$

$$b = 0$$

Figure 8 shows all W_1 data plotted against the variable x_s. The scaling is obviously much better than in Fig. 1b, which shows the same data plotted

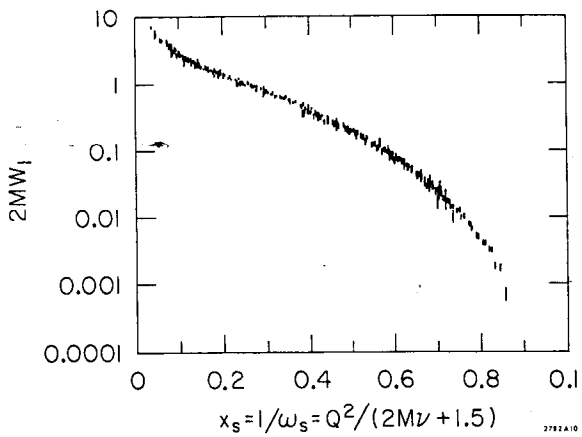

Fig. 8--Values of $2MW_1$ for the proton versus x_s, the ad hoc scaling variable. Data are included for $\epsilon \leq 0.5$, $W^2 > 4$ GeV^2, $Q^2 > $ GeV^2, $R = 0.14$.

against x. This is a demonstration that there does exist a variable in which the W_1 data scale (Atwood has also looked at the behavior of νW_2 with x_s, and this data also scales in the ad hoc variable x_s).

We can summarize the new information obtained by the two analyses by saying that both νW_2 and W_1 break scaling in x' by an amount which corresponds to a decrease in the structure functions of ~1% for an increase of Q^2 by 1 GeV^2.

C. BEHAVIOR OF THE STRUCTURE FUNCTIONS NEAR $x = 1$

Drell and Yan[11], and West[12] have suggested that the behavior of the structure functions near $x = 1$ is related to the behavior of the elastic scattering form factors. If the elastic form factors fall like $1/Q^4$ then they suggest that

$$\lim_{x \to 1} \nu W_2 \propto (1 - x)^3 \tag{10}$$

or perhaps

$$x(1 - x)^3$$

The expected behavior of $2MW_1$ is less clear:

$$\lim_{x \to 1} 2MW_1 \propto (1 - x)^3 \quad ? \tag{11}$$

Values of νW_2 were fit[13] to forms like

$$\nu W_2 = \sum_{i=n}^{i=m} \alpha_i (1 - x')^i \tag{12}$$

Good fits were obtained for $n = 3$ and $m \geq 7$. The coefficient of the cubic term, α_3, was large and positive, and this was generally interpreted as evidence favoring relation (11a). Fitting the SLAC (Group A) data in the ad hoc scaling

variable x_s:

$$W_1 = \sum_{i=3}^{i=7} \beta_i (1 - x_s)^i \tag{13}$$

gives β_3 small and consistent with zero, and a large positive value for β_4, the coefficient of $(1 - x_s)^4$. In Fig. 9 the solid dots represent the values obtained from data taken at 50° and 60°, and the open circles are values of W_1 taken from an earlier MIT-SLAC (SFG) analysis.[14] It is clear from the figure that there will be no need for significant terms in $(1 - x_s)^3$ in a fit of the form of Eq. 13. The dotted line in the figure shows how $2MW_1 \propto (1-x_s)^3$ would appear if normalized at $x_s \sim 0.5$.

Figures 10a and b show the effect of a change in variables on the leading powers. In Figure 10a, we plot $2MW_1$ vs. $(1 - x_s)$ with logarithmic scales, and vs. $(1-x)$ in Fig. 10b. Shown in both graphs are lines corresponding to terms of the third and fourth powers in the respective variables. The slope corresponding to the fourth power is clearly a good fit in 10a but not in 10b. The absence of the cubic term thus depends on the choice of variable.

The logical conclusion would appear to be that the present W_1 data offer no confirmation of Eq. 10, though the data certainly cannot be interpreted as evidence that the relationship expressed in Eq. 10 is wrong. The old "confirmation" coming from νW_2 data is now somewhat suspect, since the fits were made for data in the range $0.4 \lesssim x \lesssim 0.7$ where $x(1-x)$ is constant within $\pm$ 10%. A fit with a leading term of $x(1 - x)^4$ will therefore reproduce the data as well as one with a leading term of $(1 - x)^3$. Again, nothing <u>eliminates</u> cubic terms (which would eventually dominate at large enough Q^2), but given present data the theoretical uncertainties allow one to make a fit without cubic terms. It would be comforting theoretically to believe that νW_2 does not have a lowest order term with a smaller exponent than the corresponding term in W_1, since otherwise R will increase without limit as Q^2 increases, but, of course, there is no experimental data on any of the three quantities, R, νW_2, and W_1, in the kinematic region where such effects might be observed.

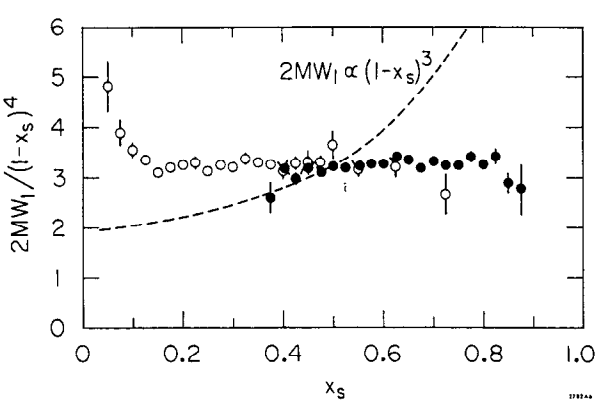

Fig. 9--$2MW_1/(1-x_s)^4$ vs. x_s. Proton data from Ref. 2 (solid circles) and Ref. 14 (open circles). The dotted lines show what would be expected if $2MW_1$ were to vary as $(1-x_s)^3$, normalized to the data at $x_s = 0.5$.

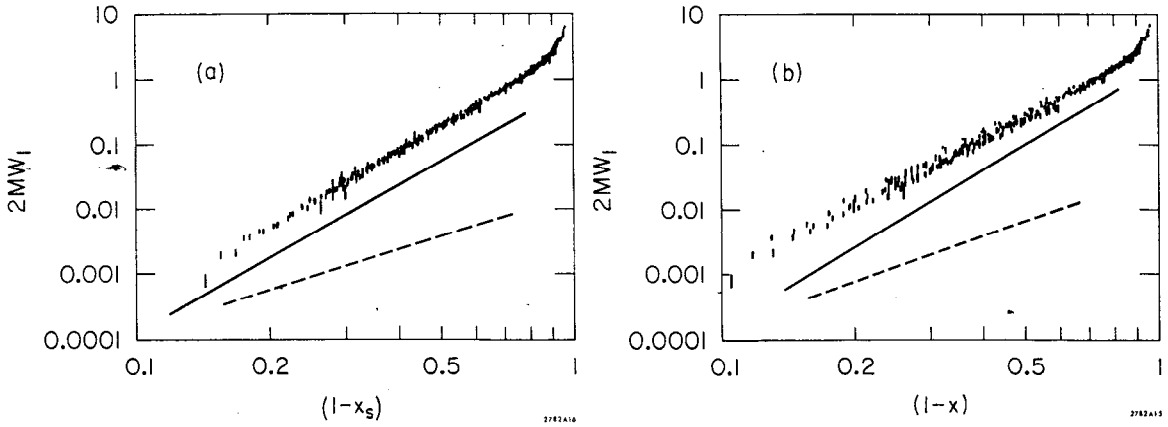

Fig. 10--Plots of $2MW_1$ vs. (a) $(1-x_s)$ and (b) $(1-x)$ from both 50° and 60° experiment and the MIT-SLAC (SFG) analysis. Points are plotted if $\epsilon \leq 1/2$, $Q^2 > \text{GeV}^2$, $W^2 > 4\ \text{GeV}^2$. The solid lines indicate a slope corresponding to $(1-x_s)$ in (a) and $(1-x)^4$ in (b) and the dotted lines show the slope of the corresponding cubic expressions.

One might consider the possibility that the structure functions behave like $(1 - x_s)^4$ and that the elastic form factor falls faster than $1/Q^4$. Figure 11 shows a recent compilation of some values of G_M obtained from measurements at SLAC. This plot includes some new data from 50° and 60°, notably two new 60° points at $Q^2 = 22\ \text{GeV}^2$ and $Q^2 = 33\ \text{GeV}^2$. As a result of background studies in the most recent experiment, a slight correction has been made

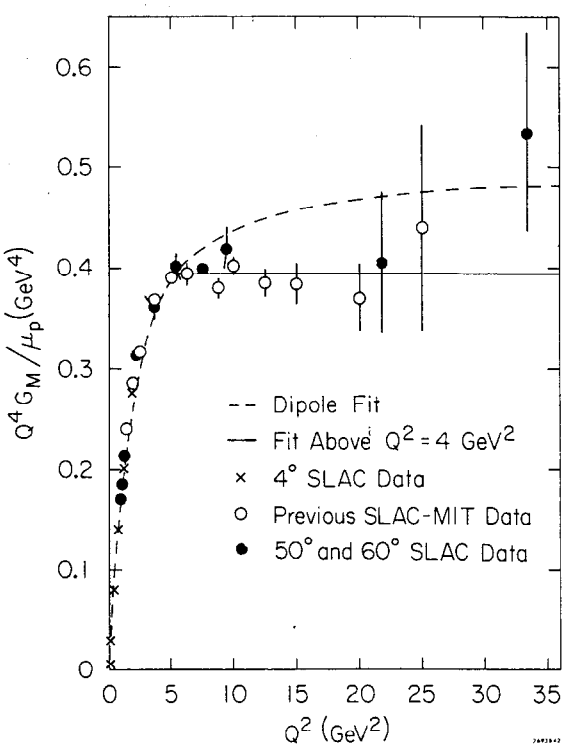

Fig. 11--Q^2 dependence of the proton form factor, G_M. Values of G_M have been extracted from elastic cross sections assuming $G_E = G_M/\mu_p$. The solid line is a fit to a constant for data above $Q^2 = 4\ \text{GeV}^2$ showing that $G_M \propto 1/Q^4$ is a good fit to the high Q^2 data.

to the $Q^2 = 25\ GeV^2$ point taken from an older experiment by the SLAC-MIT collaboration.[15] The plot shows $Q^4 G_M/\mu_p$ and illustrates that a $1/Q^4$ fall off is an acceptable fit to the data above $Q^2 = 4 GeV^2$. Note that the data fit $1/Q^4$ behavior better than the old dipole fit.

To summarize, I believe that we have no experimental support for the relations (10) and (11), nor any clear evidence that such relations could not be true. The most that can be said about the present data is that it would be taken as strong evidence for a (non-existent) theory in which fourth power behavior was expected.

D. EXPERIMENTS ON DEUTERIUM

All recent experiments have taken data on deuterium targets, along with the measurements on hydrogen. The aim of such measurements is the study of the neutron. Previous experiments have established that the scattering from the neutron is not the same as that from the proton, and it is of interest to study scale-breaking for the neutron.

MIT-SLAC (SFG) Analyses of R_d

The MIT-SLAC (SFG) group has analyzed D_2 data at each of the 75 values of (Q^2, W^2) shown in Fig. 2. Values of R_d have been determined from the deuterium cross sections using the procedure outlined above for extracting R_p. The results are shown in Fig. 12 along with the proton results. As in the proton case, several different expressions can be successfully fitted to the data. If R_d is assumed to be a constant, then a fit to all their data points

$$\bar{R}_d = 0.175 \begin{array}{ll} \pm .009 & \text{(statistical counting errors)} \\ \pm .060 & \text{(possible systematic errors)} \end{array}$$

This value is not significantly different from the value obtained for the proton

$$\bar{R}_p = 0.138 \begin{array}{l} \pm .011 \\ \pm .056 \end{array}$$

By restricting the data used in the fit to that taken using the 8-GeV spectrometer, certain systematic errors are avoided, and in this case, the authors find that the difference in the fitted constants is $.001 \pm .002$. The difference is then within the statistical counting errors.

The authors test for differences between R_d and R_p in another way by forming the ratio of σ_d/σ_p for each ϵ at each of the 75 values of (Q^2, W^2) and searching for ϵ dependence of the ratio. This is a more powerful way to search for deuterium proton differences. If $\delta = R_d - R_p = 0$, the

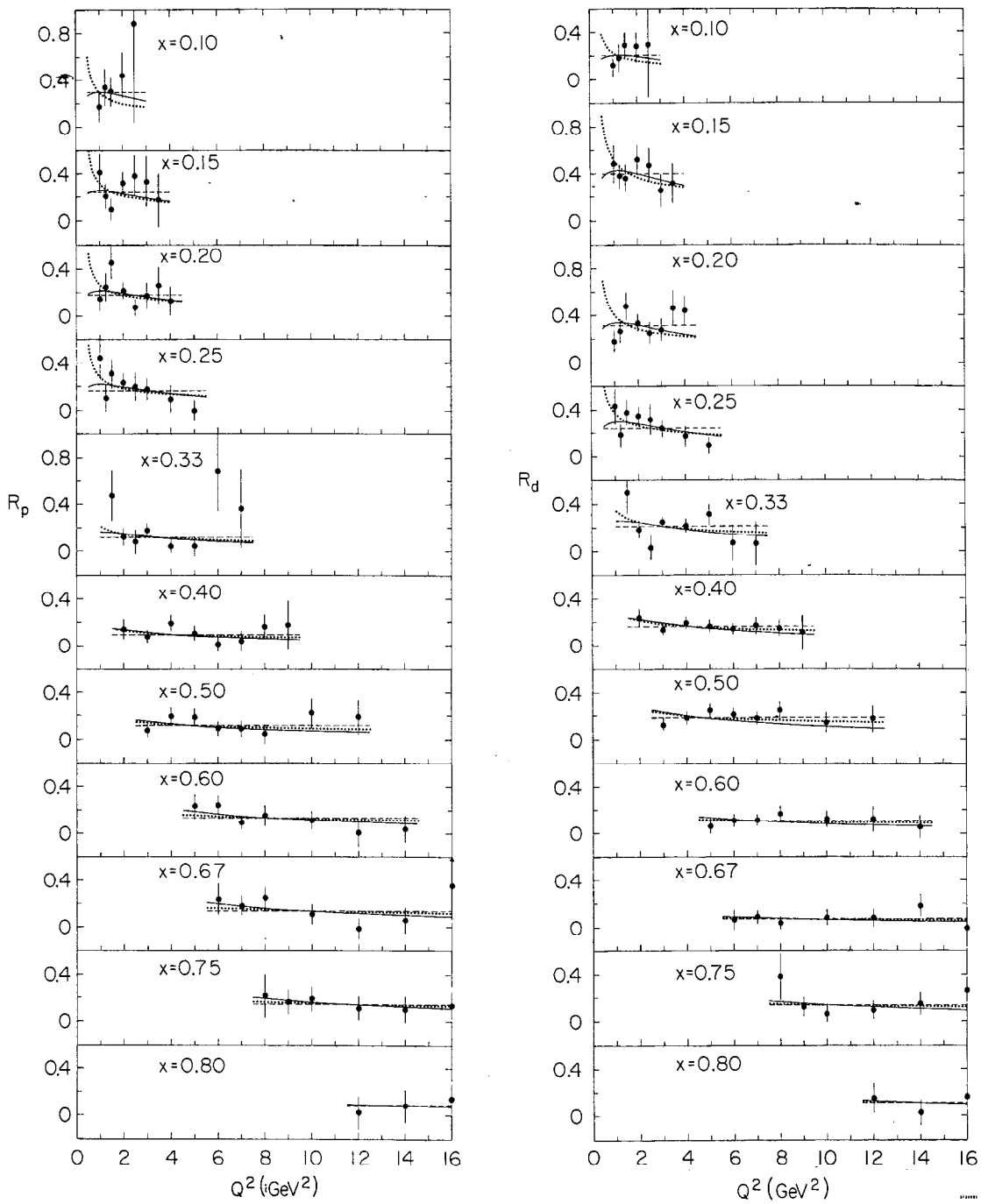

Fig. 12--Values of R_d for all 75 kinematic points in Fig. 2. Figure 3 is reproduced here to facilitate comparisons. The fits for R_d are of the same form as those in Fig. 3.

ratio of σ_d/σ_p should exhibit no ϵ dependence. Using all data they find:

$$\bar{\delta} = 0.031 \begin{array}{l} \pm .015 \text{ (statistical)} \\ \pm .036 \text{ (systematic)} \end{array}$$

and if they again restrict themselves to data taken with one spectrometer:

$$\bar{\delta}(8\text{-GeV}) = -0.001 \pm 0.022$$

and there is no need to invoke systematic errors when δ is assumed to be zero.

It is plausible that if $R_d = R_p$, then $R_n = R_p$, but the errors in R_n are obviously larger than in R_d or R_p, and our knowledge of R_n is limited. In Ref. 1, the MIT-SLAC (SFG) group note that values of R_d are somewhat smaller than R_p for $W \leq 2.5$, $x \geq 0.6$. The differences are not statistically significant, but R_n could vanish at low W without contradicting their present data. In the discussion below we assume that $R_d = R_n = R_p$.

Deuterium Structure Functions

Again, following procedures analogous to those used in the analysis of the proton data, the MIT-SLAC (SFG) group obtain 75 values of νW_2^d and $2MW_1^d$. Plots of these quantities for selected values of x are shown in Fig. 13, and the similarity to Fig. 4 is evident. Their present analysis does not fully report on the D_2 data, but they make some comments about the behavior of the deuterium cross sections in x and x'.

(1) In the variable x, scale breaking coefficients for W_1^d and νW_2^d differ from each other by ~ 2 standard deviations. The difference is much smaller if a cut is placed on the data so that $W \geq 2.6$ GeV.

(2) For $x \leq 0.3$, both proton and deuteron structure functions are consistent with scaling in x.

(3) νW_2^d is consistent with scaling in ω', W_1^d is not, but the uncertainties are such that this result is not entirely conclusive.

The significance of scaling in x' for deuterium is difficult to interpret since the proton does not scale in x'. It seems least confusing to discuss proton and neutron structure functions, even though the extraction of these functions from deuterium introduces some extra uncertainties.

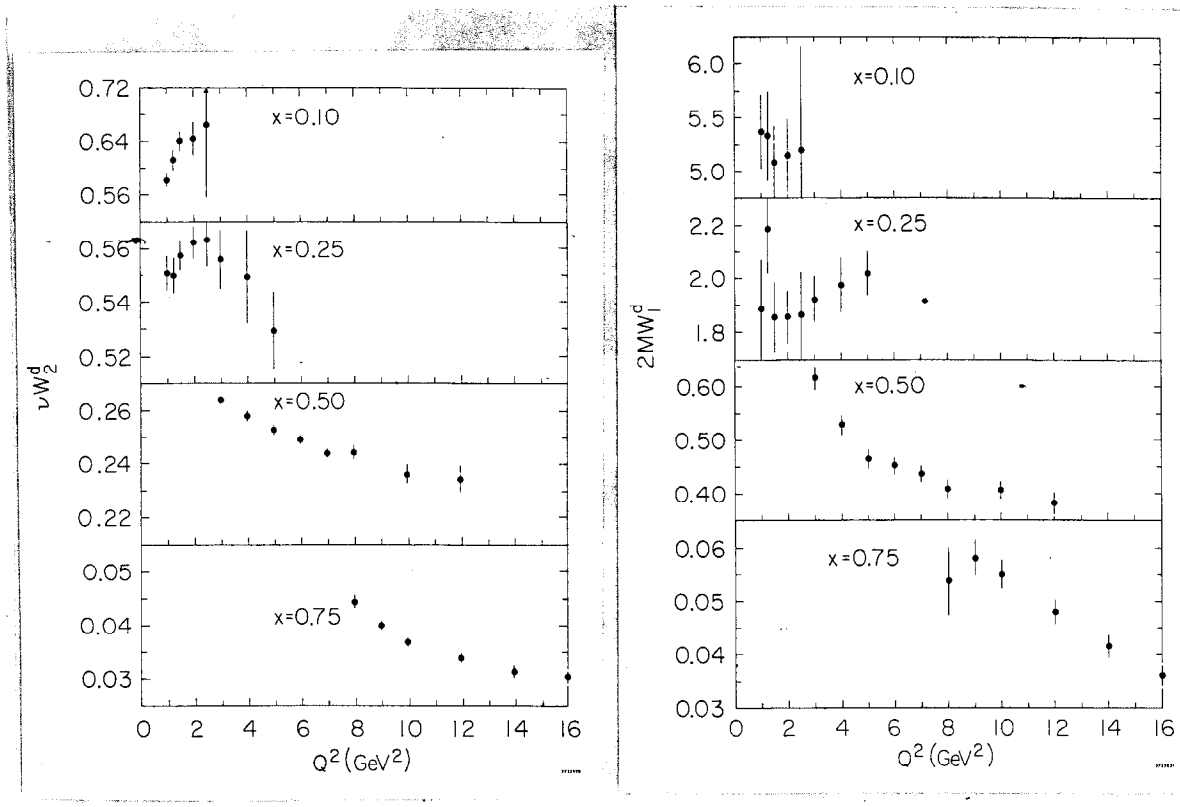

Fig. 13--νW_2^d and $2MW_1^d$ structure functions. Separated structure functions for deuterium for the same values of x as in Fig. 4.

SLAC(GROUP A) Data on Deuterium

From the deuterium data taken at 50° and 60°, values of W_1^n have been extracted, assuming that $R_n = R_p$. In some regions of the data there is an extrapolation of the $R_d = R_p$ results of the MIT-SLAC(SFG) collaboration (see Fig. 5).

Our extracted values of W_1^n scale reasonably well in x' (the coefficient b is small and consistent with zero if we use fits of the form given in Eqs. 8 and 9). Poor fits are obtained for the variables x and x_s. There is some slight conflict with the conclusions of the MIT-SLAC (SFG) group quoted above, but the actual data are not in serious disagreement.

E. SUMMARY

Table II is a summary of the information from both analyses. Fits to a combined data set have been made by Atwood for four different variables: x; x'; and the ad hoc variables

$$x_a^p = \left(\frac{1}{x} + \frac{1.5\text{GeV}^2}{Q^2}\right)^{-1} \quad (= x_s \text{ in Atwood's thesis})$$

and

$$x_a^n = \left(\frac{1}{x} + \frac{0.6\text{GeV}^2}{Q^2}\right)^{-1}$$

TABLE II

		PROTON		NEUTRON	
VARIABLE	FORM	W_1^p	νW_2^p	W_1^n	νW_2^n
x	F(x)	×	×	⊗	⁘
	$F(x)(1+bQ^2)$	×	⁘ $-0.029 \pm .001$	⊗	
x'	F(x)'	×	×		
	$F(x')(1+bQ^2)$	$-0.012 \pm .001$	$-0.011 \pm .002$	$+0.003 \pm .006$	$+0.017 \pm .008$
x_a^p $(a = 1.5\ GeV^2)$	$F(x_a^p)$			⁘	⊗
x_a^n $(a = 0.6\ GeV^2)$	$F(x_a^n)$	×	×		

× RULED OUT ⊗ PROBABLY RULED OUT ⁘ UNLIKELY

2782A34

The latter are chosen so that no scale breaking term is necessary for a good fit to W_1 data from the proton and neutron data respectively. Crosses in the table indicate that the form in the first column is a poor fit to the data for the given structure function. The judgement about what constitutes a poor fit is somewhat subjective, since the presence of systematic errors in the data interferes with the usual interpretation of X^2 in the fits. Numbers in the table are values of "b" which result in a best fit. It can be seen that the form $F(x')\ (1 + bQ^2)$ can be fitted to all four structure functions. With this form there is no discernable difference in the breaking parameters for W_1^p and νW_2^p, but there does appear to be a significant difference in the breaking between proton and neutron.

This difference between proton and neutron is seen in a different way in the bottom two rows of the table, where the ad hoc variable x_a^p enables us to fit proton data but not neutron data, and vice versa for x_a^n. One should bear in mind that these parametrizations in no way indicate that one variable is more "correct" than another, but are merely selected to illustrate how the data can be represented by various simple forms.

The difference in the scale breaking for proton and neutron indicated in Table II can be illustrated more clearly by binning W_1 over a broad range of x' in a kinematic region where corrections due to motion of the nucleons in

D_2 are small. The results for proton and neutron are shown in Fig. 14, where the difference in behavior is quite obvious.

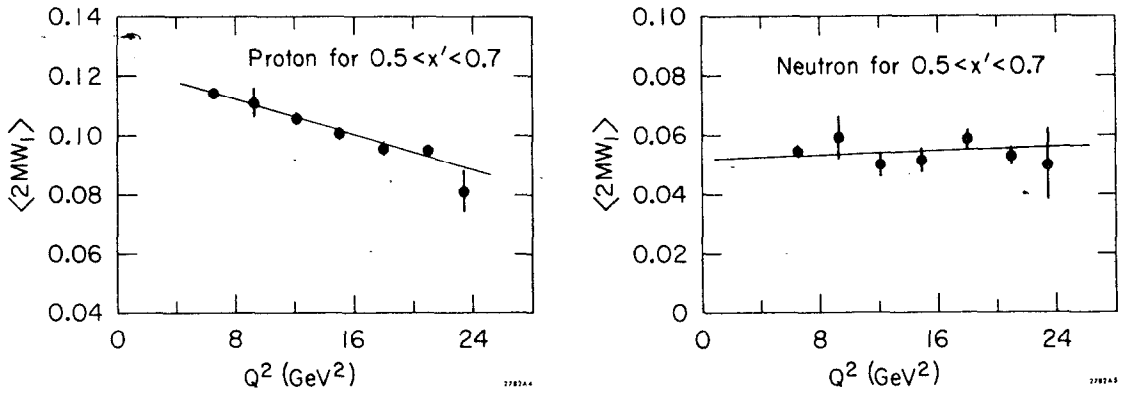

Fig. 14--Q^2 dependence of $2MW_1$. Data for (a) proton and (b) neutron from 50° and 60° in the range $0.5 < x' < 0.7$ for various Q^2. The proton data in (a) can be compared with the similar plot using the scaling variable x in Fig. 7.

F. CONCLUSIONS

(1) νW_2^p and $2MW_1^p$ do not scale in x' and break scaling in the same way. The observed breaking is not large; ~ 1% decrease in the structure function for a $1(\text{GeV})^2$ increase in Q^2.

(2) Neutron structure functions break scaling in a different manner then the proton structure functions.

(3) R_p is consistent with a constant $= 0.14 \pm .06$ (and is also consistent with $1/Q^2$ and $1/\log Q^2$ behavior).

(4) $R_d = R_p$ within experimental errors.

(5) Experimental evidence for Drell-Yan-West relations is much weaker than previously believed.

(6) Muon data from Fermilab[4] on Fe are not in conflict with electron-deuteron data where the experiments overlap in x. At small values of x the muon experiments show νW_2 <u>rising</u> with Q^2 as has been discussed in the previous talk.

III. ELECTROPRODUCTION AT LOW VALUES OF Q^2

Some recent results from a novel experiment at Cornell have been submitted to the conference.[16,17] The experiments measure electron scattering at low Q^2 with an apparatus which detects an e^- and some other particle in the reaction

$$e + A \rightarrow e' + X$$

(i.e., they detect the final electron in coincidence with one or more particles from X). Since the apparatus (Fig. 15) which detects the extra particle covers very close to 4π steradians, the efficiency for detecting events in which X includes the production of hadrons is very near 100%.

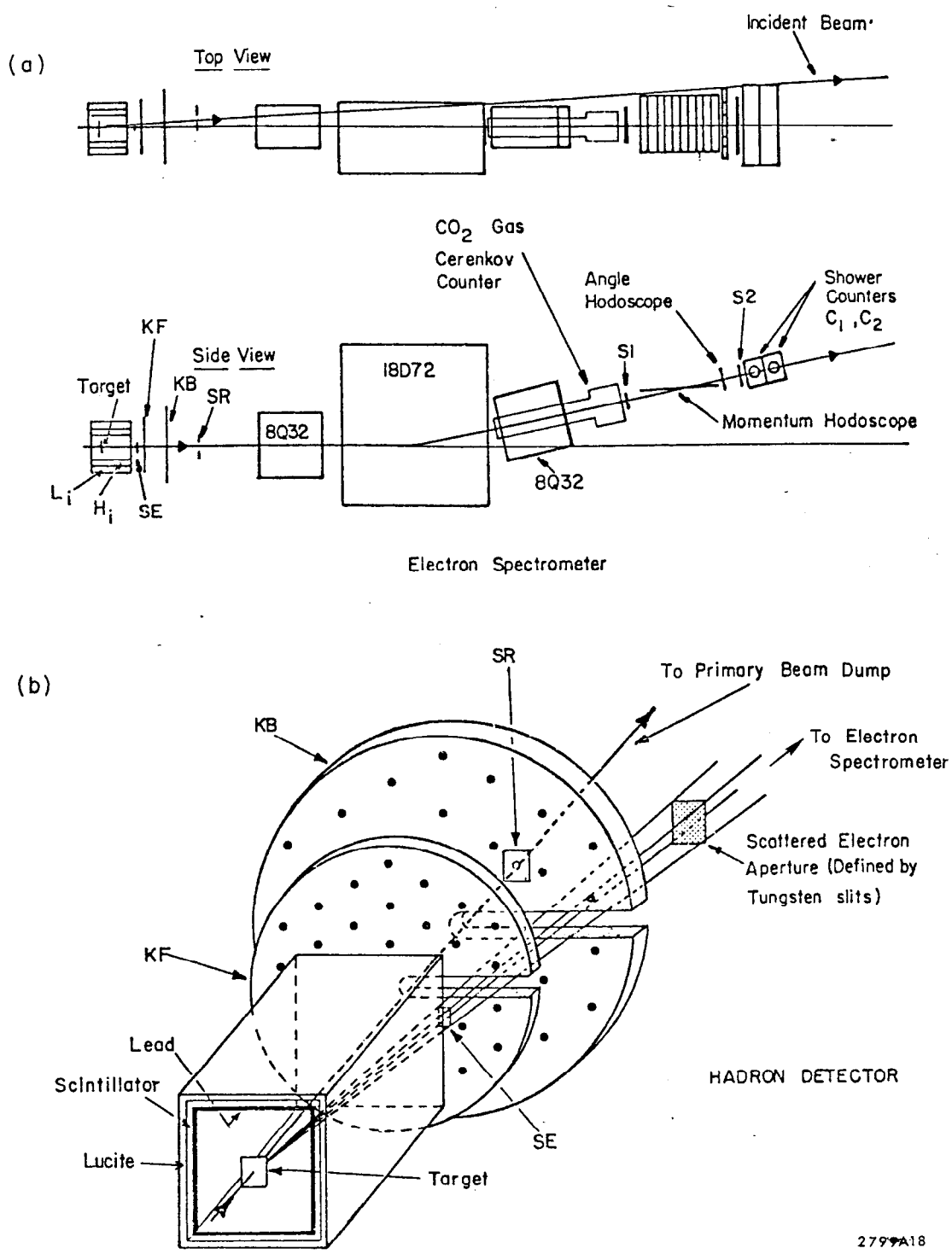

Fig. 15--Schematic of the hadron detector in Cornell experiments. Except for the "slot" containing the primary and scattered beams. The counters have a high probability for detecting hadrons produced in an inelastic scatter.

Radiative processes, on the other hand, are less likely to be observed in this apparatus since the accompanying radiation tends to peak along the direction of the incoming and outgoing electrons. A comparison of inclusive electron rates and coincidence rates from this apparatus will be a sensitive test of the radiative corrections to single-arm experiments.

The A-dependence of electroproduction is an obvious place to begin applying this technique, since radiative corrections are large for high A and low Q^2. Previous electron experiments[8,9] have been unable to detect significant A-dependence, although photon absorption experiments ($Q^2 = 0$) observe large effects. The new Cornell results[16,17] are taken at several values of ν for $Q^2 = 0.1$ GeV^2 and generally agree with the previous experiments done at SLAC. Silverman[18] has already discussed the new results in another session of this conference in terms of H, the "fraction" of the photon which exhibits hadron-like behavior (Fig. 16). Figure 17 presents the new data in a slightly different form which facilitates the comparison with other experiments.[9,18,20,21,22] There are systematic errors on both the electron data from SLAC and the muon data, which decrease the significance of the difference in behavior. From Fig. 17 it can be seen that the new Cornell data are in good agreement with the previous electron experiments, and that the new data sharpen the conflict with photoproduction results.

The second communication[17] to the conference giving results from the same apparatus deals with the behavior of the cross section for electron-deuteron scattering at low values of Q^2. To understand the interest in these measurements, a little history is perhaps appropriate. In the analysis[9] of deuterium data at 4°, Group A applied the usual[23] closure corrections to measured quasi-elastic scattering peaks. This procedure is commonly applied to such measurements and is important in the usual interpretation of the data. As an example, Fig. 18 illustrates a fit to the elastic and quasi-elastic peaks with $E_0 = 4.5$ GeV. Without the corrections calculated by Jankus, and assuming form factor scaling, the solid curve would exceed the measured points by about 15%. The question then arose as to whether similar closure corrections should be applied to the inelastic cross sections for values of $W > 1$ GeV. There is no formal justification for such a procedure if particles can be created in the scattering process (i.e., above π threshold). In the 4° data we found

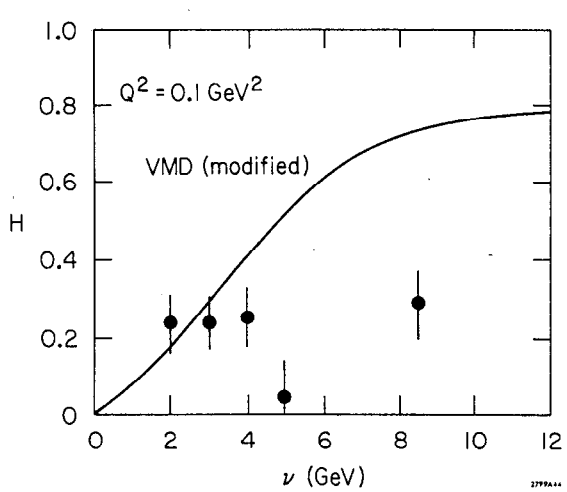

Fig. 16--Shadowing in electroproduction. A comparison of Cornell data and VMD predictions.

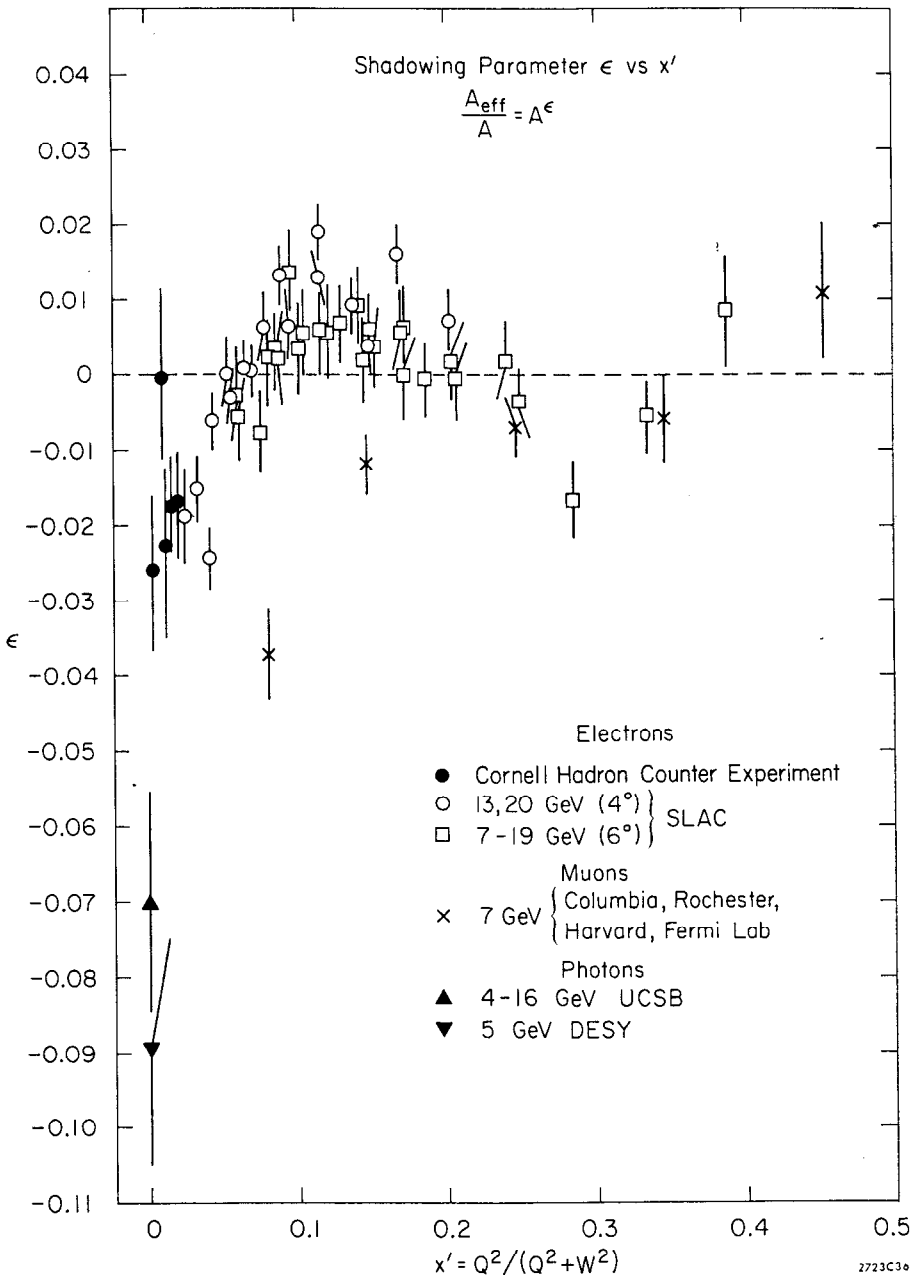

Fig. 17--Shadowing in electroproduction. A comparison of the new Cornell data with other lepto-production data and with photoproduction data. The variable x' is used for convenience. See the references for discussions of systematic errors, not all of which are included in the figure.

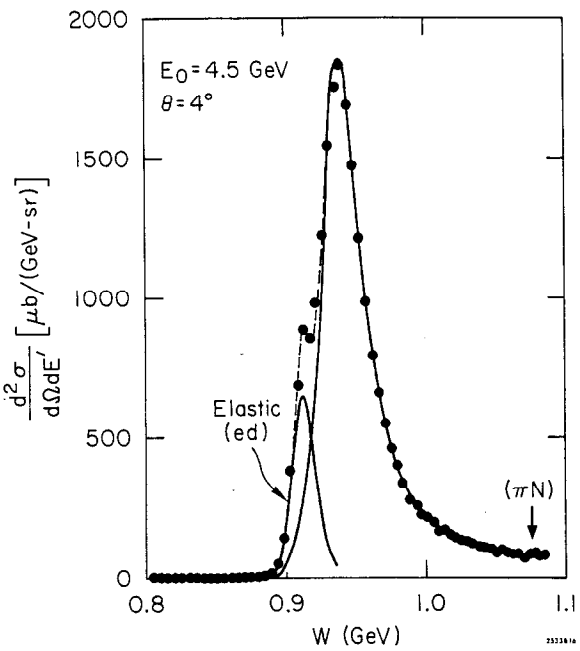

Fig. 18--Elastic and quasi-elastic scattering from deuterium. The solid curves assumes

$$G_M^n/\mu_n = G_M^p/\mu_p$$

and includes closure corrections.

some evidence of a decrease in the ratio of deuterium to hydrogen cross sections at small values of Q^2. We, therefore, applied a correction of the form

$$\sigma_D^{corrected} = \sigma_D^{measured}[1 - F_{el}^2(q^2)]^{-1}$$

to our inelastic data on D_2 before extracting a ratio of "neutron" to proton cross sections.

Cornell has extended the measurements to lower values of Q^2 and finds no evidence for a decrease in D/H ratios. Figure 19 summarizes available data

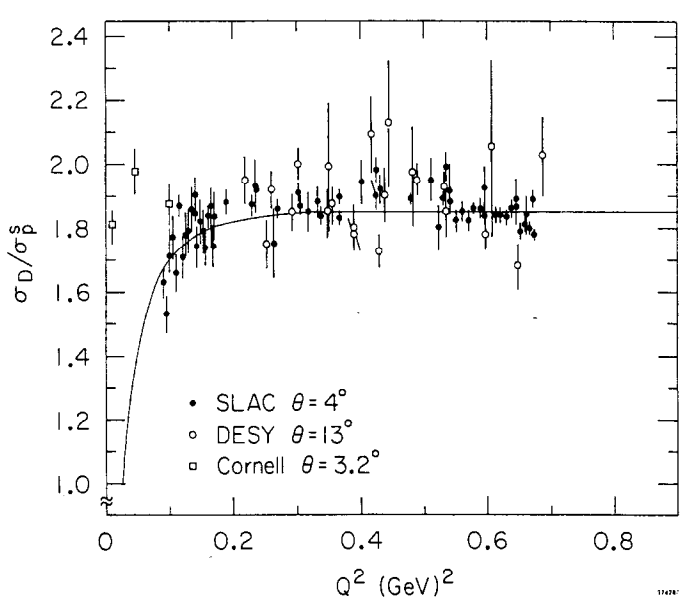

Fig. 19--Values of the ratio σ_d/σ_p^s at low Q^2 from various experiments (9,17,24). σ_p^s is derived from hydrogen measurements, folding in effects of nucleon motion and is very close to σ_p in this kinematic region. The solid line represents the behavior which would be expected if the closure approximation were correct.

on the ratios as measured by different groups.[24] The question of closure corrections to inelastic scattering assumes some practical importance when electroproduction cross sections are extrapolated to $Q^2 = 0$ in order to obtain photoproduction cross sections.

For the proton, νW_2 shows a definite fall-off at low Q^2. In analogy with the closure corrections applied to D_2 by our group, we searched for some sort of closure relation which might fit in the low Q^2 region. (A remark in the Cornell paper to the effect that the theoretical basis for this procedure is questionable plumbs the depths of understatement.) Nevertheless, we did find a parametrization (which fit the data very closely) of the form

$$\nu W_2 = F_2^p(\omega') \; [1 - W^{el}(q^2)] \tag{14}$$

where

$$W_2^{el} = \frac{G_E^2 + \tau G_M^2}{1 + \tau}$$

The new results from Cornell showing that a closure relation does not apply in the case of inelastic eD scattering presumably make it even more probable that this fit is accidental.

In a theoretical contribution to this conference[25] Devenish and Schildknecht have evaluated a particular form of generalized vector meson dominance in the "turn on" of νW_2^p. The results are compared with 4° data in Fig. 20, showing that this theory can produce acceptable fits in this Q^2 region.

IV. EXPERIMENTS WITH POLARIZED ELECTRONS

My final topic is a progress report on the work with PEGGY,[26] the polarized electron source, by a YALE-SLAC group.[27] The source, based on U.V. photoionization of a polarized Li^6 atomic beam (Fig. 21) has been operational for the past few months and has reached intensities of 2×10^9 electrons/pulse, roughly half of which are accelerated to high energies.

The Yale-SLAC collaboration has already reported the measurements of the accelerated PEGGY beam polarization[28] by Moller scattering from polarized electrons in magnetized iron at energies of 6.5, 9.7, 11.3 and 19.4 GeV. These energies correspond to various polarizations brought about by the rotation of the electron spin as the electrons pass through the magnets of the beam switchyard. The Moller scattering results are shown in Fig. 22. There is clear evidence of polarization in the accelerated beam (and, within experimental errors, no evidence of depolarization during acceleration).

The polarized beam has recently been used with a polarized target to measure the asymmetry in cross section for electron and proton spins parallel and anti-parallel.

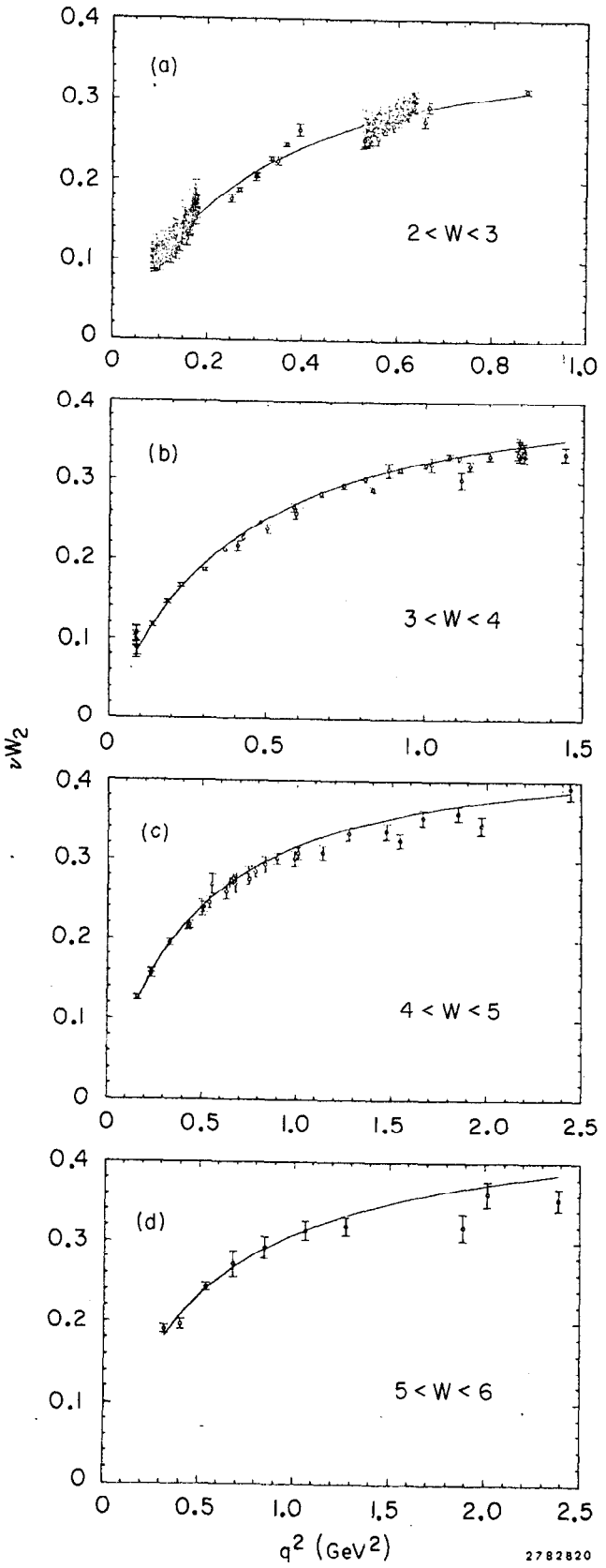

Fig. 20--Fits to νW_2^p at low Q^2 by generalized vector meson dominance theory (Ref. 25).

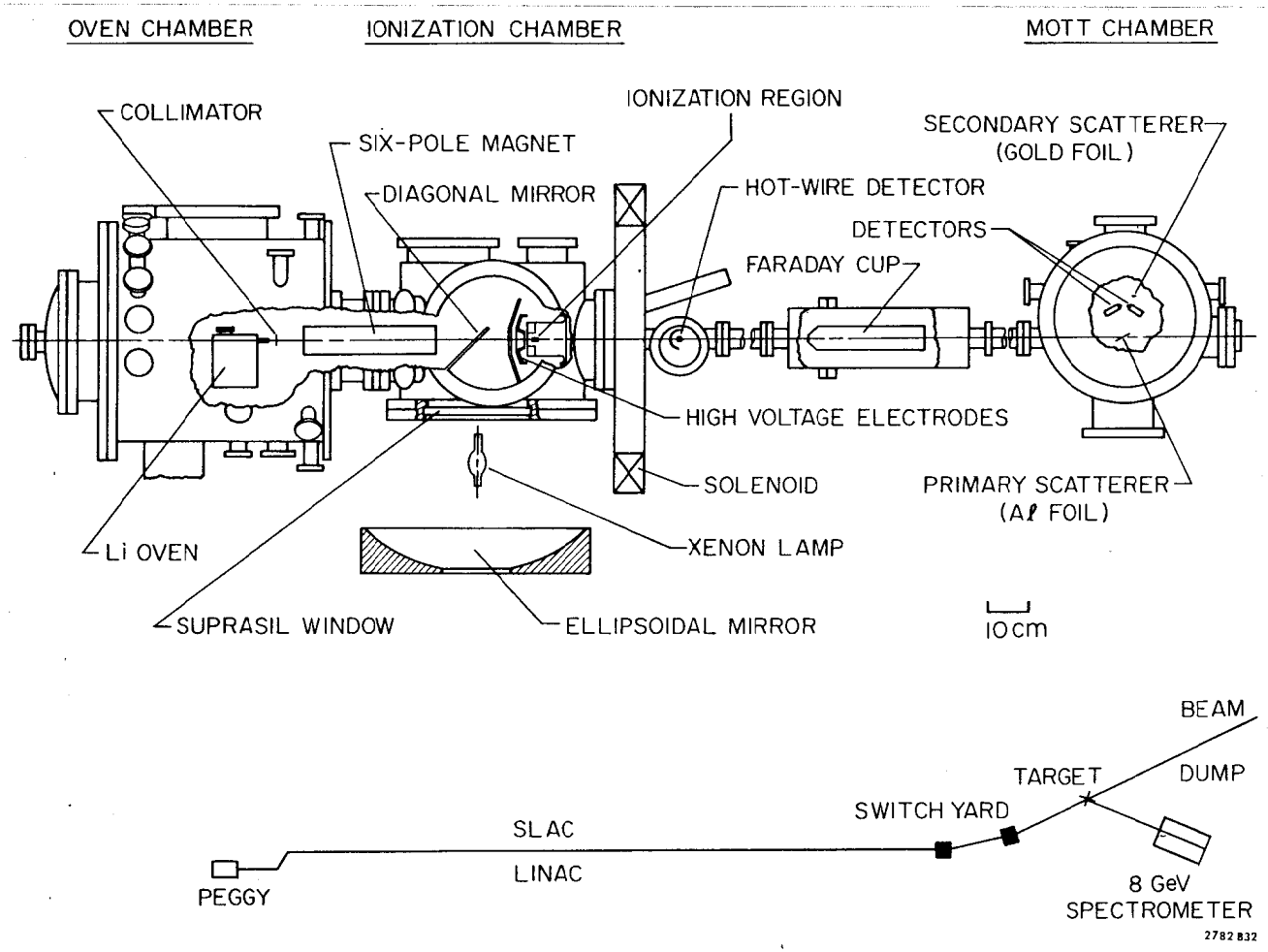

Fig. 21--Polarized electron source. A schematic view of PEGGY and some associated measuring equipment. The beam is taken off to the SLAC accelerator in the break between the hot wire detector and the Faraday Cup. Shown below is a schematic of the path of the polarized electrons through to the target in end station A.

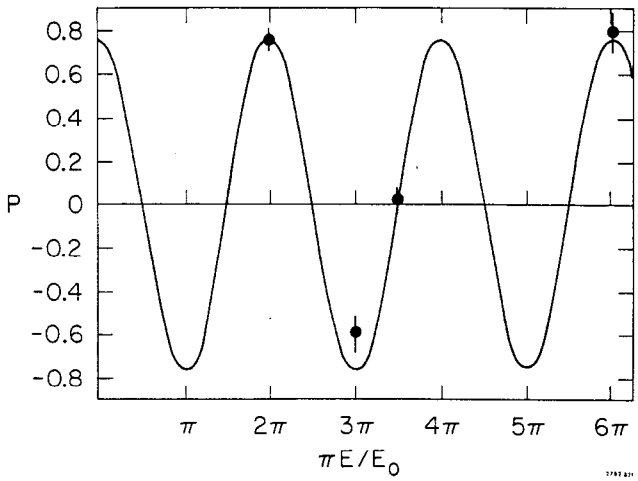

Fig. 22--Measurements of electron polarization for various energies. The solid curve is $P = P_0 \cos(\pi E/E_0)$ where E is the electron energy, P_0 is the beam polarization, and E_0 = 6.54 GeV, the beam energy at which the beam polarization would rotate by 2π radians in passing through the switchyard magnets.

For elastic scattering the asymmetry can be calculated. If A is defined as

$$A = \frac{\frac{d\sigma_A}{d\Omega} - \frac{d\sigma_P}{d\Omega}}{\frac{d\sigma_A}{d\Omega} + \frac{d\sigma_P}{d\Omega}}$$

then in elastic scattering at $\theta = 8^\circ$, $E_0 = 6.5$ GeV, the asymmetry should be +0.11. A very preliminary analysis of the present data agrees with this number to ~ 20% (only statistical errors have been considered so far).

In inelastic scattering the calculation of asymmetries is model dependent. Bjorken[29] has calculated rather large positive asymmetries on the basis of a simple quark model.

Table III shows where data has been accumulated.

The authors have had very little time to analyze this data, and at the present time, they are willing to tell us only the sign of the asymmetry in inelastic scattering, which is the same as that for elastic scattering (as expected in the quark model). More definite results will, no doubt, be announced in the near future.

TABLE III

Angle	E_0	ω	Approximate Total Counts
9°	9.7 GeV	3	10^6
9°	9.7 GeV	5	10^6
9°	12.95 GeV	3	5×10^5

ACKNOWLEDGMENTS

My thanks are due to many individuals who contributed papers to the conference. In particular, E. Riordan and J.I. Friedman of M.I.T. were of great help in making the analysis of the SLAC-MIT (SFG) collaboration available at the earliest possible moment and in spending a great deal of their time discussing the results with me.

The members of Group A at SLAC were also of great help while this talk was being prepared.

I owe thanks to my scientific secretaries, Dr. P. Kunz and Dr. W.B. Atwood. In particular, Dr. Atwood played a major role in the preparation of this talk, including many new calculations and much study and discussion of the data.

I must also acknowledge the support of the staff of SLAC Technical Publications for their untiring assistance with the figures and the assistance of Ms. M. L. Arnold.

REFERENCES

1. E. M. Riordan et al., Paper No. 252 contributed to this Symposium, SLAC-PUB-1634.

2. W. B. Atwood, Ph.D. Thesis, Electron Scattering Off Hydrogen and Deuterium at 50° and 60°, SLAC Report-185, June 1975.

3. J. D. Bjorken, Phys. Rev. Lett. 16, 408 (1966).

4. C. Chang et al., Observed Deviations from Scale Invariance in High Energy Muon Scattering, CLNS-308 or LBL-3886, July 1975.

5. G. Miller, Ph.D. Thesis, Inelastic Electron Scattering at Large Angles, SLAC Report-129, January 1971.

6. L. N. Hand, Proceedings XVII International Conference on High Energy Physics, p. IV-61, London, 1974.

7. L. W. Mo, Invited Paper at this Symposium.

8. F. Gilman, Invited Paper at this Symposium.

9. S. Stein et al., Electron Scattering at 4° with Energies of 4.5-20 GeV, SLAC-PUB-1528, 1975. Phys. Rev. D12, 1884 (1975).

10. The MIT-SLAC (SFG) group actually use a slightly different form instead of Eq. 9, viz.,

$$F_1(\omega_a) = \frac{1}{x_a} \sum_{i=3}^{i=7} \alpha_i (1 - x_a)^i$$

11. S. D. Drell and T. M. Yan, Phys. Rev. Letters 24, 181 (1970).

12. G. B. West, Phys. Rev. Letters 24, 1206 (1970).

13. G. Miller et al., Phys. Rev. D5, 528 (1972).

14. a) A. Bodek et al., Proceedings XVII International Conference on High Energy Physics, p. IV-57, London, 1974.

b) E. M. Riordan, Ph.D. Thesis, An Experimental Study of the Nucleon Structure Functions, MIT (1973) Report # LNS-COO-3069-176.

c) E. M. Riordan et al., Phys. Letters 52B, 249 (1974).

15. P. N. Kirk et al., Phys. Rev. D, 8, 63 (1973).

16. J. Eickmeyer et al., Paper No. 216 contributed to this Symposium.

17. J. Eickmeyer et al., Paper No. 217 contributed to this Symposium.

18. W. R. Ditzler et al., Phys. Lett. 57B, 201 (1975).

19. A. Silverman, Invited Paper at this Symposium.

20. M. May et al., University of Rochester Report UR-532, May 1975.

21. D. O. Caldwell et al., Phys. Rev. D7, 1362 (1973).

22. V. Heyen et al., Phys. Lett. 34B, 651 (1971).

23. V. Z. Jankus, Phys. Rev. 102, 1586 (1956).

24. The graph includes new data points from DESY, J. Bleckwenn et al., Paper No. 273 contributed to this Symposium.

25. R. C. E. Devenish et al., DESY 75/18, July 1975.

26. M. J. Alguard et al., Proceedings of the IX International Conference on High Energy Accelerators--SLAC, p. 309 (1974).

27. M. J. Alguard et al., Paper No. 160 contributed to this Symposium.

28. P.S. Cooper et al., Phys. Rev. Lett. 34, 1589 (1975).

29. J. D. Bjorken, Phys. Rev. D1, 1376 (1970).